Krokos George (Orcid ID: 0000-0001-7428-0066)
Papadopoulos Vassilis, P. (Orcid ID: 0000-0001-5877-5149)
Dybczak Patryk, Albert (Orcid ID: 0000-0002-8685-2057)
Hoteit Ibrahim (Orcid ID: 0000-0002-3751-4393)

Natural Climate Oscillations May Counteract Red Sea Warming over the Coming Decades

George Krokos[1], Vassilis P. Papadopoulos[2], Sarantis S. Sofianos[3], Hernando Ombao[4], Patryk Dybczak[4], Ibrahim Hoteit[1]

[1]Physical Science & Engineering Division, King Abdullah University of Science and Technology, Thuwal, Saudi Arabia

[2]Hellenic Centre for Marine Research, Anavissos, Greece

[3]Division of Environmental Physics, University of Athens, Athens, Greece

[4]Computational, Electrical and Mathematical Science and Engineering, King Abdullah University of Science and Technology, Thuwal, Saudi Arabia

Corresponding authors: Ibrahim Hoteit (Ibrahim.hoteit@kaust.edu.sa), George Krokos (georgios.krokos@kaust.edu.sa)

Key Points:

- The Red Sea SST exhibits long-term oscillations related to the Atlantic Multidecadal Oscillation.
- High warming trends for the period 1980-2010 are dominated by a positive phase of the natural SST oscillation.
- SST over the Red Sea is expected to shift to a cooling phase during the next few decades.

Abstract

Recent reports of warming trends in the Red Sea raise concerns about the response of the basin's fragile ecosystem under an increasingly warming climate. Using a variety of available Sea Surface Temperature (SST) datasets, we investigate the evolution of Red Sea SST in relation to natural climate variability. Analysis of long-term SST datasets reveals a sequence of alternating positive and negative trends, with similar amplitudes and a periodicity of nearly 70 years associated with the Atlantic Multidecadal Oscillation (AMO). High warming rates reported recently appear to be a combined effect of global warming and a positive phase of natural SST oscillations. Over the next decades, the SST trend in the Red Sea purely related to global warming is expected to be counteracted by the cooling AMO phase. Regardless of the current positive trends, projections incorporating long-term natural oscillations suggest a possible decreasing effect on SST in the near future.

Plain Language Summary

The recent warming trend of the Red Sea SST is critical for the fragile basin's ecosystem, especially for its precious coral reef community. Several studies based on satellite-era datasets recently reported warming rates that can rapidly alter the environmental status of the Red Sea in the near future. We show that the long-term variation of the SST over the Red Sea is influenced by a natural oscillation related to the Atlantic Multidecadal Oscillation (AMO). Satellite-era datasets coincide with a positive phase of this oscillation and the associated SST trend is overstated compared to the real, long term trend. As AMO currently shifts from positive to negative phase, the Red Sea SST is expected to shift into a cooling phase during the next decades.

1 Introduction

The marginal, semi-enclosed Red Sea hosts a diverse marine ecosystem ornamented by a rich coral reef community that is highly vulnerable to changes in water temperature (Cantin et al., 2010). Repetitive exposure to heat stress is considered amongst the most critical threats to coral reef communities, and could lead to mass coral bleaching events (Hughes et al., 2018). Recently, a number of studies have indicated that the Red Sea coral reefs have been significantly affected by bleaching caused by strong heat waves (Kotb et al., 2004; Furby et al., 2013; Osman et al., 2018). Because of their relatively small volume and the slow rate of their water renewal, marginal semi-enclosed seas such as the Red Sea, are more susceptible to global warming. In a benchmark study of the warming rate of large marine ecosystems, Belkin (2009) reported a worldwide rapid warming from 1982 to 2006. During the same period, the Red Sea also displayed evidence of significant warming (Raitsos et al., 2011; Chaidez et al., 2017). As one of the warmest oceanic basins on the planet, a further increase of the sea water temperature could be critical for the Red Sea marine ecosystem.

During the 20th century, the majority of Earth's oceans have showed an increasing trend in sea surface temperature (SST), with signs of intensification in the last few decades (Ting et al., 2009; Large & Yeager, 2012; Reid & Beaugrand, 2012). Most of these studies were performed over short time periods during which the warming rates could be hindered or intensified by natural, longer-term variability. For example, analysis of long-term SST datasets suggested that this was the case for the adjacent Mediterranean Sea (Marullo et al.,

2011; Macias et al., 2013). In those studies, an oscillation with a periodicity of about 70 years was reported for the Mediterranean SST long-term variability. The sinusoidal SST variation was linked to the Atlantic Multidecadal Oscillation (AMO), a natural oscillation defined by the anomaly of the average SST over the north Atlantic (Richard A Kerr, 2000). Macias et al. (2013) reported that during the AMO positive phase, the human-induced warming rates in the Mediterranean for the period 1980-2005 may be overestimated due to the associated SST oscillation.

Although AMO has been reported to affect the neighboring Mediterranean Sea (Marullo et al., 2011), its influence on the long-term Red Sea SST variability remains unclear. In this study, we use four available SST datasets to investigate the SST evolution in the Red Sea and its potential relation to the AMO natural oscillation. We examine the reported high warming rates of the Red Sea SST, taking into account the long-term natural SST variability, which we use as a basis to provide future projections.

2 Datasets and methods

2.1 SST datasets

The temporal variability of SST in the Red Sea is investigated using four datasets of different time spans and spatial resolutions. Two modern-era satellite products, used in recent studies to assess the recent Red Sea SST trends (Chaidez et al., 2017; Raitsos et al., 2011), and two long-term reconstruction datasets were selected. The first dataset was provided by the National Oceanic and Atmospheric Administration (Reynolds et al., 2007) on a 0.25 degree grid, with a daily resolution spanning a period from 1981 to present. This specific product (AVHRR-OI) is the longest available single instrument, remotely-sensed dataset. The second is the operational SST and Sea Ice Analysis (OSTIA), provided by the UK Met Office (Donlon et al., 2012). OSTIA uses a blend of satellite data, together with in-situ observations from the International Comprehensive Ocean-Atmosphere Data Set (ICOADS) database. The analysis produces daily SST fields at 0.05 degrees resolution spanning the period 1985 to present.

For the long-term analysis, we used two SST reconstructions: the NOAA's extended Reconstructed Sea Surface Temperature [ERSST] and the Hadley Centre Sea Ice and Sea Surface Temperature [HadISST]. The ERSST dataset is a global monthly SST analysis on a 2°×2° grid that covers the period 1854-2018 (Smith & Reynolds, 2003; Smith et al., 2008). The specific version ERSST v5 uses new data from the recently released ICOADS 3.0 dataset and Argo floats, and does not include satellite data. The HadISST dataset was provided by the UK MetOffice on a 1° grid and covers the period 1870-2018 on a monthly resolution (Rayner, 2003). The dataset is based on in situ observations from the Met Office Marine Data Bank (MDB) and the ICOADS dataset; it also includes satellite data from the post-1985 period. Being a strategic shipping route, the Red Sea enjoys continuous observations in the historical datasets.

2.2 Atlantic Multidecadal Oscillation index

AMO, first identified by Schlesinger and Ramankutty (1994), is a natural long-term climate cycle defined by the SST patterns in the North Atlantic Ocean that exhibit a periodicity of 60-80 years (Kerr, 2000). Recent studies have shown that the AMO is a permanent feature of the climate system, associated with variations in the Atlantic conveyor belt that has been shown to exist on millennial time scales (R. A. Kerr, 2005; Knight et al., 2006). The AMO has been linked to important climate impacts, such as the multidecadal variability of the North American and European summer climate and the northern

hemispheric mean surface temperature (Sutton & Hodson, 2005; Knight et al., 2006; Marullo et al., 2011). The AMO time series used in this study is a linear detrended, unsmoothed index based on the Kaplan SST dataset (Kaplan et al., 1998).

2.3 Singular Spectral Analysis (SSA)

Singular spectral analysis (SSA) is used to identify the dominant modes of variability in a time series (Ghil et al., 2002). It is a powerful tool for identifying oscillatory components in dynamical systems (Vautard et al., 1992). The concept of SSA relates to the decomposition of the original series into independent and interpretable components and its noise. The method is based on the principal component analysis (PCA), but more adaptable to various time scales and provides a better qualitative decomposition from short and noisy time series. SSA is implemented here to identify and reconstruct the dominant frequency signals. The method is applied to both averaged SST over the Red Sea and to individual basin-wide grid points for examining the spatial structure of SST variability (see also Section S2 in Supporting Information).

2.4 Linear regression model

The reconstructed time series resulting from the SSA analysis and the estimated linear trends were used as a basis statistical model (described in details in Section S3 of Supporting Information). A sinusoidal function, fitted to the reconstructed low frequency signal of the SSA analysis, was used to represent the identified oscillatory signal. A linear regression model was then considered as a function of the linear trend and the oscillatory component. To account for persistence in the residuals of the initial model, we followed a general least square (GLS) approach (Shumway & Stoffer, 2017). An autoregressive modeling (AR) method was used to update the model and obtain estimates with white noise errors. An ordinary least squares method was then used to fit the updated model and obtain confidence intervals for the expected future SST.

3. Results and Discussion

3.1 Recent SST trends (Satellite era) in the Red Sea

An assessment of the recent trends and spatial patterns of SST evolution in the Red Sea is performed by comparing the SST reconstructions during the satellite era (1985 to present), for which data are available from all datasets. The annual evolution of the basin average SST and the related trends for each dataset are presented in Figure 1 (upper panel). Although the mean SST values vary between the different datasets, which mainly reflects the limited spatial coverage of the coarse resolution datasets, they are generally consistent in terms of interannual variability and trends, which is the focus of the present study.

A noticeable feature during the satellite-era period is a warming trend of about 0.2°C per decade (0.29°C for ERSSTv5), which is clear in all datasets, despite the differences in data sources and resolutions. Furthermore, all datasets suggest that the warming trend exhibits a North-South gradient, with higher warming rates in the Northern Red Sea (Figure 1 – lower panel). This is consistent with the findings of Chaidez et al. (2017), who reported a similar trend for maximum annual temperatures in the Red Sea, more prominent in the northern part of the basin. These spatial patterns are better captured by the two high-resolution datasets (AVHRR-OI, OSTIA), but are also pronounced in the lower resolution (HadSST, ERSSTv5) products. Langodan et al. (2017) reported a gradual reduction of wind strength during the last decades over the Northern Red Sea, which is consistent with the warming SST trend. This emphasizes the connection between the variability of the prevailing atmospheric forcing and the climatic changes observed in the broader region.

3.2. Long-term SST variability

The annual mean SST time series, averaged over the entire Red Sea, over the period 1875-2015 are presented in Figure 2. The period prior to 1875 (before the opening of the Suez Canal) was not considered in our analysis due to limitations in the available in-situ measurements, and the consequently reduced performance of the SST reconstructions. The two independent long-term SST products used in this study describe a similar evolution of SST in terms of inter-annual variability and trends, consistent with Marullo et al. (2011) results in the Mediterranean Sea. Hereafter, we focus our analysis on the higher resolution HadISST dataset, which provides a better representation of the spatial structure of the SST variability in the Red Sea.

Regardless of the abruptness of the recent-era trends, the long-term analysis reveals a significantly lower (~0.04 °C/decade) overall warming compared to the trends inferred using only the satellite era datasets (~0.2 °C/decade); although, indeed, the last two decades is the warmest period the Red Sea has experienced. Fourier analysis of the annual SST time series averaged over the Red sea (Section 1 and Figure S1 in Supporting Information), reveals a dominant frequency in the power spectrum of ~70 years, suggesting a sequence of alternating positive and negative trends. In Figure 3 (upper panel), the annual mean SST time series, averaged over the whole Red Sea, are split into four periods of 35 years, each corresponding to successive phases of warming and cooling SST trends (Figure 3 – lower panel). A North-South gradient was observed in both cooling and warming phases, with higher rates in the Northern Red Sea. A multidecadal oscillation, similar to that identified in the Red Sea, has also been reported for the Mediterranean Sea and the Atlantic Ocean (e.g. Artale et al., 2006). This similarity may be attributed to the extensive atmospheric teleconnection affecting a large part of the Northern Hemisphere. A 70-year oscillation was also identified by Felis et al. (2000) who analyzed coral reef growth in the Northern Red Sea, based on a 245 year coral oxygen isotope record. The study also provided evidence of the relation of coral growth to SST variability and argued about the Atlantic origin of the observed SST variability and the eventual relationship to the AMO. Because the AMO has its origin in the North Atlantic region, an atmospheric teleconnection is most likely through the Northern part of the basin. Indeed, the northern Red Sea is mostly affected by climatic indices based mainly on the large scale atmospheric circulation that originates in the North Atlantic (Abualnaja et al., 2015; Papadopoulos et al., 2013; Viswanadhapalli et al., 2016).

3.3. AMO and Red Sea SST

Artale et al. (2002) and Marullo et al. (2011) suggested a clear effect of the North Atlantic regime on the Mediterranean Sea, expressed by the climatic indices North Atlantic Oscillation (NAO) and AMO. As the AMO exhibits a periodicity of around 70 years, studies based on short-term datasets (e.g. limited to the satellite era) cannot detect potential links with long-term natural climate oscillations.

To assess if a similar AMO-related oscillation affects the Red Sea SST, we performed SSA on the annual average time series over the basin (Section S2 in Supporting Information). Examination of the AMO-related temporal modes reveals that they account for a significant part of the Red Sea SST variability. The dominant pair of modes clearly show the existence of a low frequency oscillation that has a mean period of about 70 years, while their variance explains ~30% of its total interannual variability. SSA was then applied to the AMO time series. As expected, we found the dominant modes of the climate index to be representative of an oscillation of approximately 70 years (explaining ~55% of its variability), in agreement with previous studies that estimated the period of AMO between 60–80 years (e.g. Schlesinger & Ramankutty, 1994; Delworth & Mann, 2000).

When the AMO index and the annual mean SST are reproduced using only their dominant modes derived by the SSA, the two reconstructed time series exhibit a very high correlation (0.91), with a lag of six years. The results, in which HadSST time series were shifted to account for the correlation lag (for straightforward comparison), are presented in Figure 4 (upper panel). In order to examine the spatial structure of the AMO related variability, the SSA analysis was then performed separately for each grid point of the HadISST dataset in the Red Sea and the adjacent Gulf of Aden. The results, in terms of variance explained by the associated modes, correlation with the AMO signal, and the associated lags are presented in Figure 4 (lower panel). In most cases, the modes associated to AMO were dominant, accounting for an important part of the SST long-term variability. However, higher frequency oscillations prevailed in regions like the South-Central Red Sea. The accumulated energy, which expresses the percentage of variability of the modes used for the reconstruction, is presented in Figure 4a. Similar to the spatial patterns of the recent trends mentioned earlier, the dominant signal is observed in the Northern Red Sea, with accumulated energy gradually decreasing, from 55% in the North to 15% in the South.

The correlation coefficients between the SST and AMO filtered signals are presented in Figure 4b, and the related correlation lags in Figure 4c. The correlations are higher in the North and weaken towards the Southern Red Sea. However, despite the southward reduction in the energy of the related modes, the correlations exhibit high values also in the Southern Red Sea and the Gulf of Aden. Similarly, the correlation lags suggest a decoupling between the Northern and Southern Red Sea.

The high correlation in the Northern Red Sea, and the minimum phase shift (1-3 years) of the oscillation signal, suggest a direct influence of the AMO signal, probably of atmospheric origin, through the eastern Mediterranean. Despite the relatively small variability explained in the South, the correlation also suggests an influence from the AMO signal. The Southern Red Sea is strongly affected by water exchanges with the Indian Ocean (Yao et al., 2014; Dreano et al., 2016; Sofianos & Johns, 2015). Since the effects of AMO have also been shown to extend to the Indian Ocean (Marullo et al., 2011), we hypothesize that the AMO influence may propagate by advection through the Gulf of Aden into the Southern Red Sea, and the significantly higher correlation lag (~10-11 years) may correspond to the time needed for the propagation of the AMO signal.

3.4 Future projections

Based on the agreement between the long-term oscillation frequency of AMO and the Red Sea SST, and given the evidence of AMO on millennial timescales (Kerr, 2005), we statistically project the low frequency signal of the Red Sea SST over the next decades. In our analysis we consider that the long-term trend and the interdecadal oscillations, revealed by the spectral analysis, are decoupled and thus act independently. Therefore, the AMO related modes are treated here as the factor representing the natural dynamical system, whereas the contribution of climate change is represented by its long-term trend.

Following a GLS approach (described in details in Section S3 of Supporting Information), we generated a future projection of the low-frequency SST variability (Fig. 5). The projection represents the combined effect of the low frequency signal associated with the AMO and the identified long-term trends, bounded by pointwise 95% confidence intervals.

Assuming that the long-term trend due to global warming remains constant over the next decades, and not accounting for (yet to be explored) the potential impacts of climate change on the regularity of the AMO variability, the current average temperature is projected to decrease and remain below the current average temperatures during the negative phase of

the AMO oscillation (next 3-4 decades). Nonetheless, the analysis reveals that long-term trends identified in the Red Sea may be masked by the negative phase of the AMO over the next decades. A rebound of SST to new extremes is then expected to follow during the next positive phase of the AMO, reflecting the combined effect of the long-term trend and the positive phase of the identified oscillation.

4. Conclusions

Analysis of different datasets of SST in the Red Sea confirms the short-term increasing alarming trends that have been reported in recent studies. We provide strong evidence suggesting that these trends are modulated by the existence of a long-term oscillation related to AMO, with a period of approximately 70 years. The reported trends for the Red Sea based on recent-era satellite datasets indeed overlap with a positive phase of the AMO. Thus, the warming trends during this period (1980-2010), although legitimate in absolute warming rates, are the combination of both global warming and a positive phase of the natural climate cycle. Hitherto, the effects of natural climatic variability, manifested in the Red Sea as low frequency oscillations that follow the AMO oscillation, have been dominant over the identified long-term trends.

The AMO is projected to enter in a negative phase, after reaching its peak over the past decade. Given the estimated lag in the response of the Red Sea SST, the current period should exhibit the highest annual mean temperatures following the AMO peak. Based on our projection of the evolution of the SST in the near future, depending on the intensity and continuity of global warming, we expect a decreasing trend in SST. Assuming that global warming pace remains at current rates, the projected negative phase of AMO could overshadow its influence for a period corresponding to the half of the AMO cycle (approximately 35 years). In other words, the negative phase of AMO is very likely to mask the global warming effect and temporarily mitigate the consequent impacts on the Red Sea. However, the warming signal associated with climate change will continue to affect the local SST, while a rebound of temperatures to new extremes is expected to follow in the next positive phase of the oscillation.

Acknowledgments, Samples, and Data

The study was supported by King Abdullah University of Science and Technology (KAUST) under the "Virtual Red Sea Initiative", Award Number REP/1/3268-01-01. We acknowledge all data providers that made their datasets available for this study, and specifically thank the UK MetOffice Ocean for providing the OSTIA and HadISST products, NASA for providing the AVHRR-OI data, and NOAA for providing the ERSST data and the AMO time series. The SSA analysis was performed with routines developed in Matlab by Eric Breitenberger. We are also grateful to Dionysios Raitsos, John Gittings and Sabique Langodan for the valuable discussions during the preparation of the manuscript.

References

Abualnaja, Y., Papadopoulos, V. P., Josey, S. a, Hoteit, I., Kontoyiannis, H., & Raitsos, D. E. (2015). Impacts of Climate Modes on Air–Sea Heat Exchange in the Red Sea. *Journal of Climate*, *28*(7), 2665–2681. https://doi.org/10.1175/JCLI-D-14-00379.1

Artale, V., Calmanti, S., & Sutera, A. (2002). Thermohaline circulation sensitivity to

intermediate-level anomalies. *Tellus, Series A: Dynamic Meteorology and Oceanography*, *54*(2), 159–174. https://doi.org/10.1034/j.1600-0870.2002.01284.x

Artale, V., Calmanti, S., Malanotte-Rizzoli, P., Pisacane, G., Rupolo, V., & Tsimplis, M. (2006). *The Atlantic and the Mediterranean Sea as connected systems*.

Belkin, I. M. (2009). Rapid warming of Large Marine Ecosystems. *Progress in Oceanography*, *81*(1–4), 207–213. https://doi.org/10.1016/j.pocean.2009.04.011

Cantin, N. E., Cohen, A. L., Karnauskas, K. B., Tarrant, A. M., & McCorkle, D. C. (2010). Ocean Warming Slows Coral Growth in the Central Red Sea. *Science*, *329*(5989), 322–325. https://doi.org/10.1126/science.1190182

Chaidez, V., Dreano, D., Agusti, S., Duarte, C. M., & Hoteit, I. (2017). Decadal trends in Red Sea maximum surface temperature. *Scientific Reports*, *7*(1), 8144. https://doi.org/10.1038/s41598-017-08146-z

Delworth, T., & Mann, M. E. (2000). Observed and simulated multi decadal variability in the Northern Hemisphere. *Clim. Dyn.*, *16*, 661–676. https://doi.org/10.1007/s003820000075

Donlon, C. J., Martin, M., Stark, J., Roberts-Jones, J., Fiedler, E., & Wimmer, W. (2012). The Operational Sea Surface Temperature and Sea Ice Analysis (OSTIA) system. *Remote Sensing of Environment*, *116*, 140–158. https://doi.org/10.1016/j.rse.2010.10.017

Dreano, D., Raitsos, D. E., Gittings, J., Krokos, G., & Hoteit, I. (2016). The gulf of aden intermediate water intrusion regulates the southern Red Sea summer phytoplankton blooms. *PLoS ONE*, *11*(12). https://doi.org/10.1371/journal.pone.0168440

Felis, T., Pätzold, J., Loya, Y., Fine, M., Nawar, A. H., & Wefer, G. (2000). A coral oxygen isotope record from the northern Red Sea documenting NAO, ENSO, and North Pacific teleconnections on Middle East climate variability since the year 1750. *Paleoceanography*, *15*(6), 679–694. https://doi.org/10.1029/1999PA000477

Furby, K. A., Bouwmeester, J., & Berumen, M. L. (2013). Susceptibility of central Red Sea corals during a major bleaching event. *Coral Reefs*, *32*(2), 505–513. https://doi.org/10.1007/s00338-012-0998-5

Ghil, M., Allen, M. R., Dettinger, M. D., Ide, K., Kondrashov, D., Mann, M. E., et al. (2002). Advanced spectral methods for climate time series. *Reviews of Geophysics*, *40*(1), 3.1-3.41. https://doi.org/10.1029/2001RG000092

Hughes, T. P., Anderson, K. D., Connolly, S. R., Heron, S. F., Kerry, J. T., Lough, J. M., et al. (2018). Spatial and temporal patterns of mass bleaching of corals in the Anthropocene. *Science*, *359*(6371), 80–83. https://doi.org/10.1126/science.aan8048

Kaplan, A., Cane, M. A., Kushnir, Y., Clement, A. C., Benno Blumenthal, M., & Rajagopalan, B. (1998). Analyses of global sea surface temperature 1856-1991. *Journal of Geophysical Research*, *103589*(15), 567–18. https://doi.org/10.1029/97JC01736

Kerr, R. A. (2000). A North Atlantic Climate Pacemaker for the Centuries. *Science*, *288*(5473), 1984 LP-1985. Retrieved from

http://science.sciencemag.org/content/288/5473/1984.abstract

Kerr, R. A. (2005). CLIMATE CHANGE: Atlantic Climate Pacemaker for Millennia Past, Decades Hence? *Science*, *309*(5731), 41–43. https://doi.org/10.1126/science.309.5731.41

Knight, J. R., Folland, C. K., & Scaife, A. A. (2006). Climate impacts of the Atlantic multidecadal oscillation. *Geophysical Research Letters*, *33*(17), 2–5. https://doi.org/10.1029/2006GL026242

Kotb, M., Abdulaziz, M., Al-Agwan, Z., Alshaikh, K., Al-Yami, H., Banajah, A., et al. (2004). Status of Coral Reefs in the Red Sea and Gulf of Aden in 2004. *Status of Coral Reefs of the World 2002*, *1*(May 2015), 137–151. Retrieved from http://www.gcrmn.org/status2004.aspx

Langodan, S., Cavaleri, L., Vishwanadhapalli, Y., Pomaro, A., Bertotti, L., & Hoteit, I. (2017). The climatology of the Red Sea – part 1: the wind. *International Journal of Climatology*, *37*(13), 4509–4517. https://doi.org/10.1002/joc.5103

Large, W. G., & Yeager, S. G. (2012). On the observed trends and changes in global sea surface temperature and air-sea heat fluxes (1984-2006). *Journal of Climate*, *25*(18), 6123–6135. https://doi.org/10.1175/JCLI-D-11-00148.1

Macias, D., Garcia-Gorriz, E., & Stips, A. (2013). Understanding the causes of recent warming of mediterranean waters. How much could be attributed to climate change? *PLoS ONE*, *8*(11). https://doi.org/10.1371/journal.pone.0081591

Marullo, S., Artale, V., & Santoleri, R. (2011). The SST multidecadal variability in the Atlantic-Mediterranean region and its relation to AMO. *Journal of Climate*, *24*(16), 4385–4401. https://doi.org/10.1175/2011JCLI3884.1

Osman, E. O., Smith, D. J., Ziegler, M., Kürten, B., Conrad, C., El-Haddad, K. M., et al. (2018). Thermal refugia against coral bleaching throughout the northern Red Sea. *Global Change Biology*, *24*(2), e474–e484. https://doi.org/10.1111/gcb.13895

Papadopoulos, V. P., Abualnaja, Y., Josey, S. a., Bower, A., Raitsos, D. E., Kontoyiannis, H., & Hoteit, I. (2013). Atmospheric Forcing of the Winter Air–Sea Heat Fluxes over the Northern Red Sea. *Journal of Climate*, *26*(5), 1685–1701. https://doi.org/10.1175/JCLI-D-12-00267.1

Raitsos, D. E., Hoteit, I., Prihartato, P. K., Chronis, T., Triantafyllou, G., & Abualnaja, Y. (2011). Abrupt warming of the Red Sea. *Geophysical Research Letters*, *38*(14), n/a-n/a. https://doi.org/10.1029/2011GL047984

Raitsos, D. E., Yi, X., Platt, T., Racault, M., Brewin, R. J. W., Pradhan, Y., et al. (2015). Monsoon oscillations regulate fertility of the Red Sea. *Geophysical Research Letters*, n/a-n/a. https://doi.org/10.1002/2014GL062882

Rayner, N. A. (2003). Global analyses of sea surface temperature, sea ice, and night marine air temperature since the late nineteenth century. *Journal of Geophysical Research*, *108*(D14), 4407. https://doi.org/10.1029/2002JD002670

Reid, P. C., & Beaugrand, G. G. (2012). Global synchrony of an accelerating rise in sea surface temperature. *Journal of the Marine Biological Association of the United Kingdom*, *92*(7), 1435–1450. https://doi.org/10.1017/S0025315412000549

Reynolds, R. W., Smith, T. M., Liu, C., Chelton, D. B., Casey, K. S., & Schlax, M. G. (2007). Daily high-resolution-blended analyses for sea surface temperature. *Journal of Climate*, *20*(22), 5473–5496. https://doi.org/10.1175/2007JCLI1824.1

Schlesinger, M. E., & Ramankutty, N. (1994). An oscillation in the global climate system of period 65–70 years. *Nature*, *367*(6465), 723–726. https://doi.org/10.1038/367723a0

Shumway, R. H., & Stoffer, D. S. (2017). *Time Series Analysis and Its Applications*. Cham: Springer International Publishing. https://doi.org/10.1007/978-3-319-52452-8

Smith, T. M., & Reynolds, R. W. (2003). Extended reconstruction of global sea surface temperatures based on COADS data (1854-1997). *Journal of Climate*, *16*(10), 1495–1510. https://doi.org/10.1175/1520-0442-16.10.1495

Smith, T. M., Reynolds, R. W., Peterson, T. C., & Lawrimore, J. (2008). Improvements to NOAA's historical merged land-ocean surface temperature analysis (1880-2006). *Journal of Climate*, *21*(10), 2283–2296. https://doi.org/10.1175/2007JCLI2100.1

Sofianos, S., & Johns, W. E. (2015). *The Red Sea: Water Mass Formation, Overturning Circulation, and the Exchange of the Red Sea with the Adjacent Basins*. (N. M. A. Rasul & I. C. F. Stewart, Eds.). Berlin, Heidelberg: Springer Berlin Heidelberg. https://doi.org/10.1007/978-3-662-45201-1

Sutton, R. T., & Hodson, D. L. R. (2005). Atlantic Ocean Forcing of North American and European Summer Climate. *Science*, *309*(5731), 115–118. https://doi.org/10.1126/science.1109496

Ting, M., Kushnir, Y., Seager, R., & Li, C. (2009). Forced and internal twentieth-century SST trends in the North Atlantic. *Journal of Climate*, *22*(6), 1469–1481. https://doi.org/10.1175/2008JCLI2561.1

Vautard, R., Yiou, P., & Ghil, M. (1992). Singular-spectrum analysis: A toolkit for short, noisy chaotic signals. *Physica D: Nonlinear Phenomena*, *58*(1–4), 95–126. https://doi.org/10.1016/0167-2789(92)90103-T

Viswanadhapalli, Y., Dasari, H. P., Langodan, S., Challa, V. S., & Hoteit, I. (2016). Climatic features of the Red Sea from a regional assimilative model. *International Journal of Climatology*. https://doi.org/10.1002/joc.4865

Yao, F., Hoteit, I., Pratt, L. J., Bower, A. S., Köhl, A., Gopalakrishnan, G., & Rivas, D. (2014). Seasonal overturning circulation in the Red Sea: 2. Winter circulation. *Journal of Geophysical Research: Oceans*, *119*(4), 2263–2289. https://doi.org/10.1002/2013JC009331

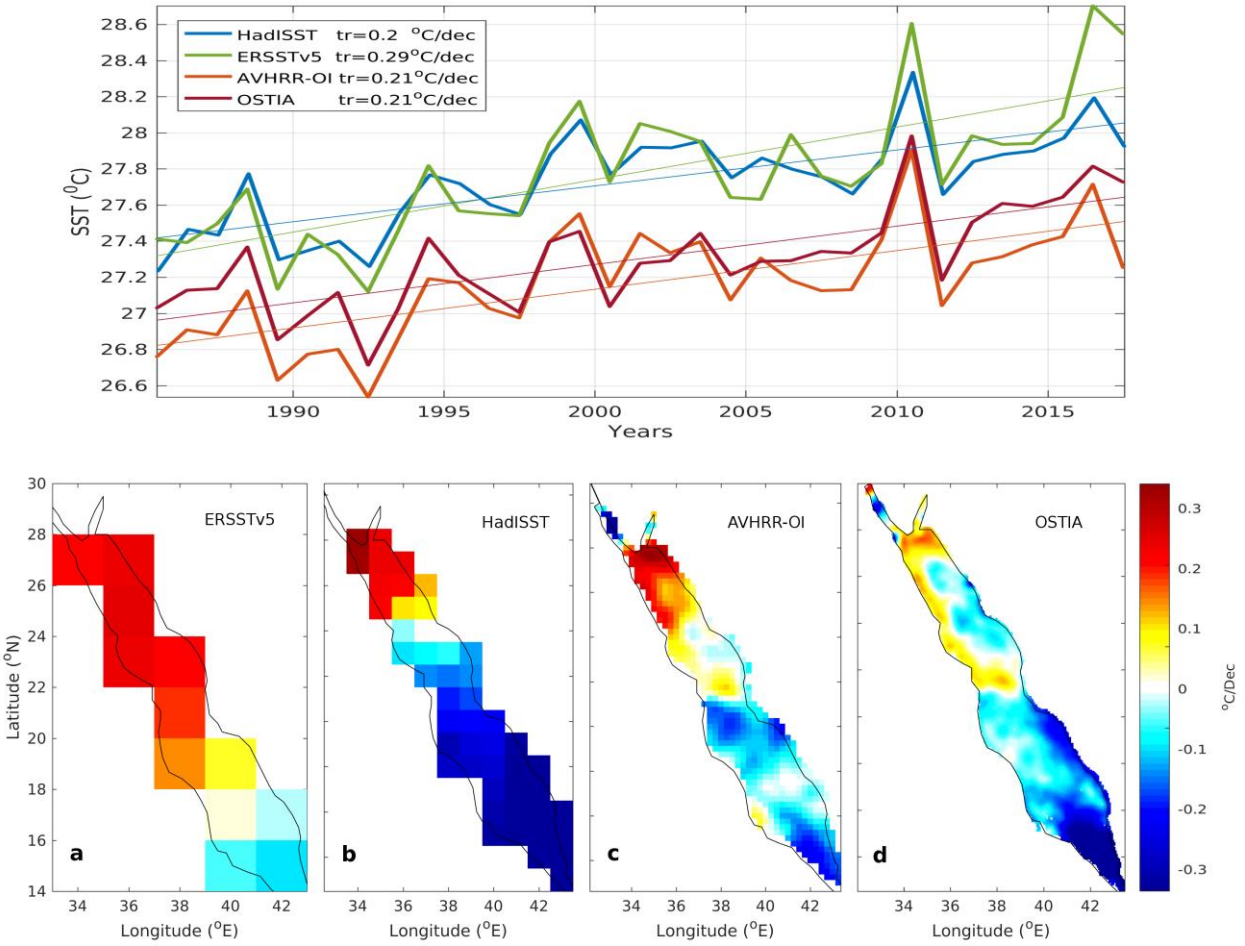

Figure 1. Upper panel: Annual mean SSTs and their respective linear trends, over the1985-2015 period. Lower panel: Spatial patterns of linear trends of SST in the Red Sea, for each examined dataset over the 1985-2015 period (a. ERSST, b. HadISST, c. AVHRR, d. OSTIA).

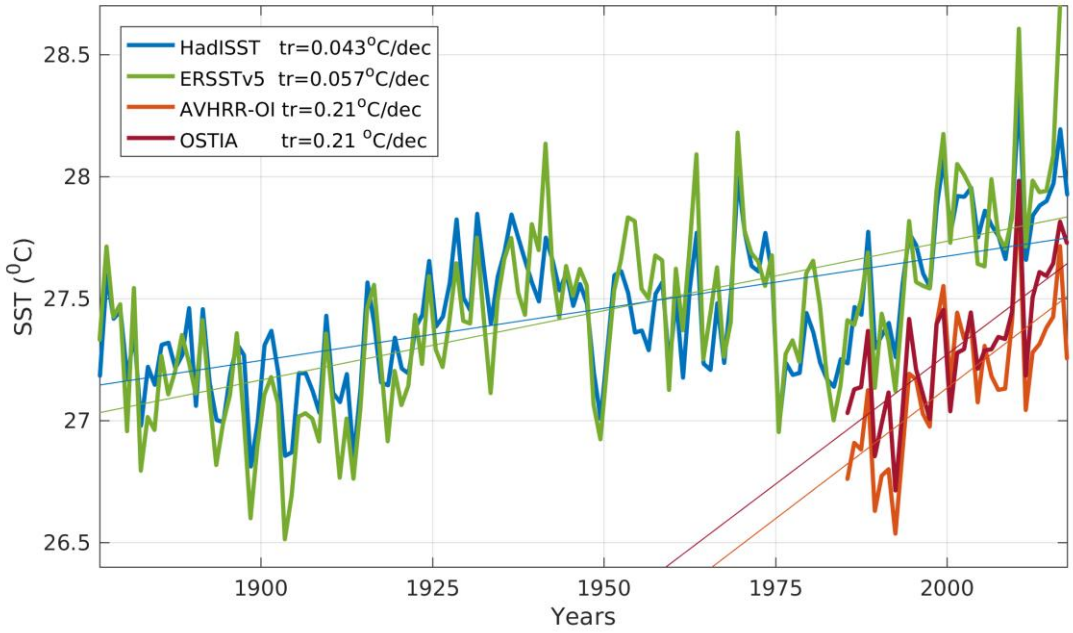

Figure 2. Annual mean SSTs and their respective linear trends, based on the full length of the considered datasets: 1880-2015 for HadISST, 1880-2015 for ERSST, 1985-2015 for the two satellite SST products, AVHRR-OI and OSTIA.

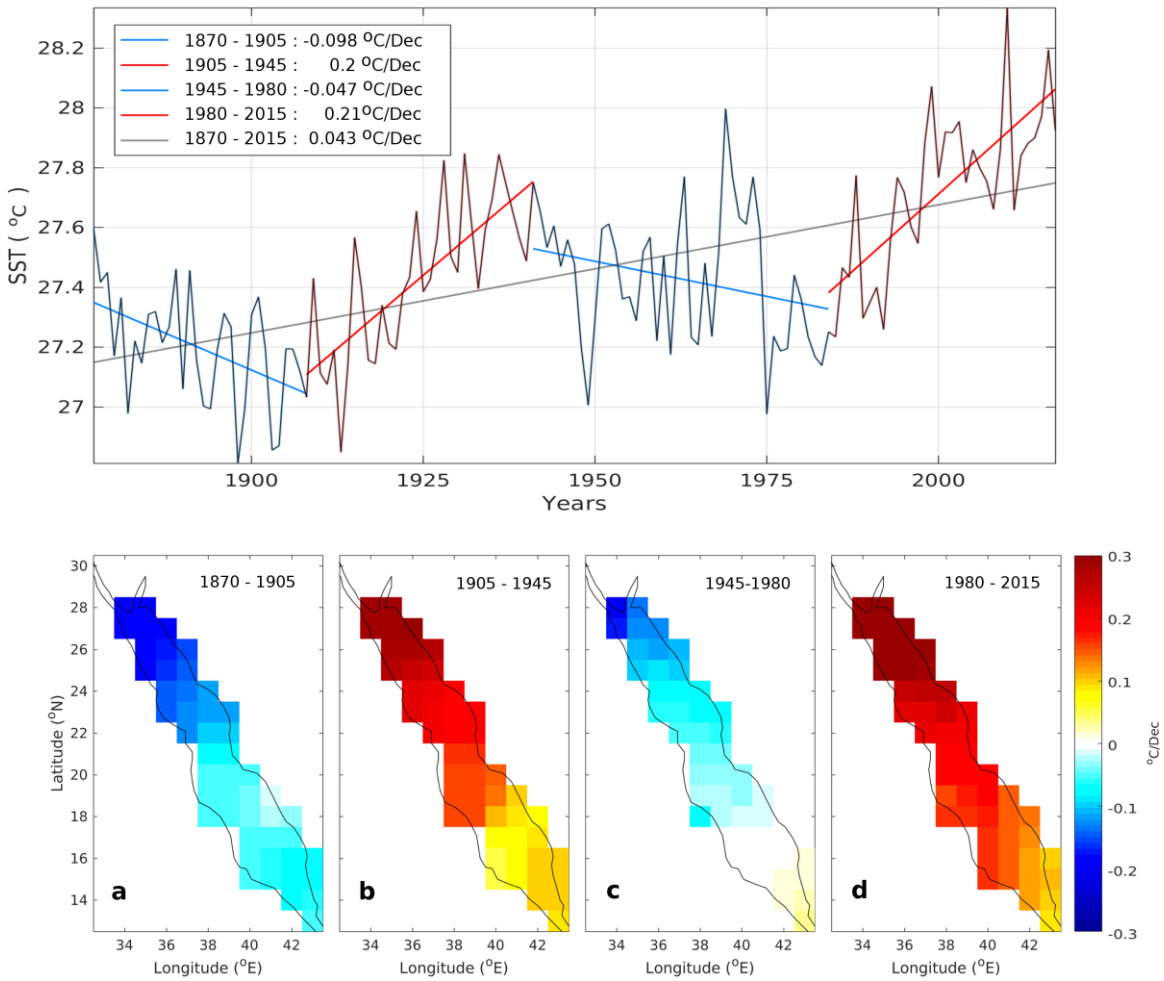

Figure 3. Upper panel: Annual mean SST, based on the HadISST dataset over the Red Sea, for the period 1880-2015, with the identified positive (red lines) and negative (blue lines) trends. Lower panel: The respective spatial patterns of the linear trends computed for each period.

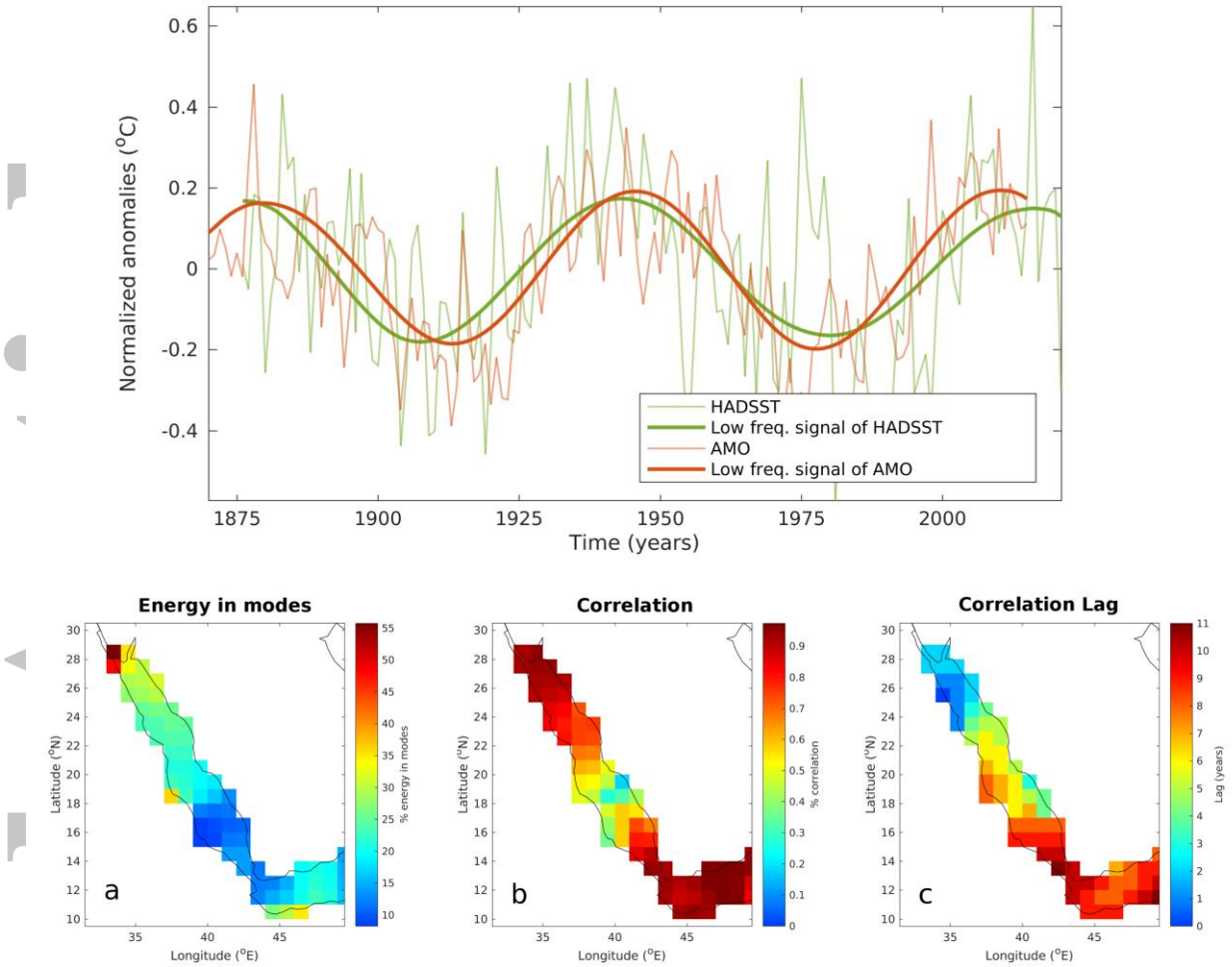

Figure 4. Upper panel: Normalized anomalies of the de-trended annual means of the Red Sea SST (HadISST, thin green line) versus AMO index (thin red line), and their low- frequency signals obtained by the SSA analysis (thick red and green lines respectively). Lower panel: Maps of accumulated energy in the low frequency modes of HadISST that are associated with the AMO (a), their correlation with the respective modes of AMO (b) and their corresponding correlation lags (c).

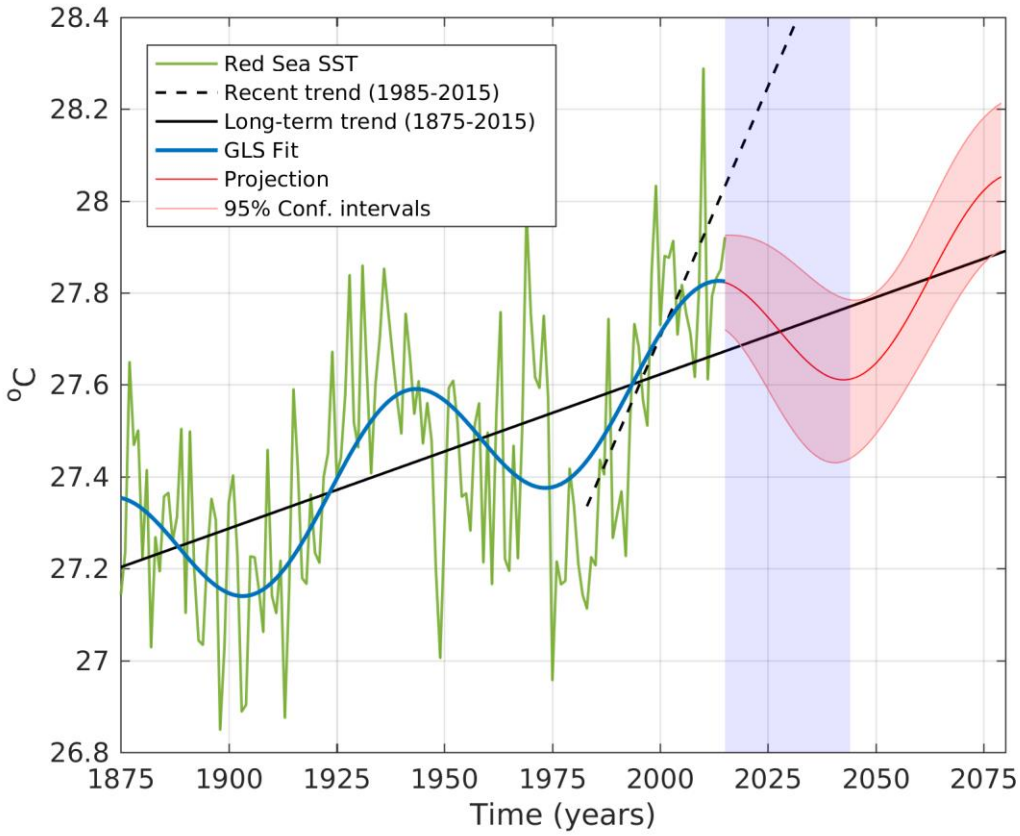

Figure 5. Projection of SST time series based on the superposition of linear trends and the low- frequency AMO signal (red line), bounded by the 95% confidence intervals (shaded red areas). The annual mean SST is shown in green. The solid black line represents trends based on the historical period (1880-2015); the dotted black line represents trends based on the satellite era (1985-2015). The shaded blue area highlights the period of the projected negative trends.